ORIGINAL PAPER

Mechanical Properties and Constitutive Model of Red Sandstone Under Acid Corrosion

Yongsheng Liu[1] · Wang Liu[1,2] · Cui Wang[2]

Abstract In order to investigate the deterioration pattern of red sandstone under acidic environment, the porosity and mechanical parameters of red sandstone specimens at different stages under different pH corrosion were measured by physical tests and uniaxial compression tests, and the effects of pH and corrosion time on the porosity and mechanical parameters of red sandstone specimens were investigated. Based on the changed in secondary porosity of red sandstone specimens after acid corrosion, chemical damage variables were introduced, and a mathematical function of chemical damage variables and mechanical parameters was established. Based on the characteristics of the uniaxial compression stress–strain curve and the Lemaitre strain equivalence principle, combined with the Weibull distribution statistical damage model for micro-fractures and porosity changed after acid corrosion, and considered the effect of the compression-tight stage, the constitutive model of the red sandstone was obtained by segmentation. The theoretical constitutive curve is compared with the test curve to check the reasonableness of the constitutive model.

Keywords Acid corrosion · Red sandstone · Porosity · Mechanical properties · Constitutive model

Introduction

As society becomes more industrialised, the corrosive effects of atmospheric acid rain on buildings are becoming increasingly apparent [1]. Acid corrosion causes changes in the microstructure and mineral composition of the rock, affecting its mechanical properties and posing a major challenge to the stability of the project [2–4].

Based on compression tests, Han et al. [5, 6] investigated the changes in the mechanical properties of granite under corrosion by different chemical solutions and analysed the damage mechanism of the mechanical properties of granite after corrosion by chemical solutions. Mei et al. [7] studied the deterioration of mechanical parameters of rock fracture surfaces after chemical corrosion and concluded that fracture surface friction and bonding properties were significantly reduced after acid corrosion. Huang et al. [8] studied the patterns of variation in the damage of granite, sandstone and marble under coupled conditions of chemical and temperature. Li et al. [9] studied the pattern of variation of the mechanical parameters and the damage characteristics of sandstone under uniaxial compression.

The above studies have laid a good foundation for our understanding of the mechanical properties of rocks under chemical corrosion. In recent years, with the continuous development of statistical mechanics, many scholars have carried out further research on rock constitutive theory and proposed many rock constitutive theories, which provide us with broad ideas to study the mechanical properties of rocks [10–14].

Based on damage mechanics and the Mohr–Coulomb strength criterion, Ji et al. [15] developed a damage constitutive model for rocks under uniaxial compression and verified the adequacy of the model by comparing the theoretical and experimental curves. Li et al. [16] analysed the

✉ Wang Liu
2020019081400003@ecjtu.edu.cn

1 School of Civil Engineering and Architecture, East China Jiaotong University, Nanchang, China

2 Department of Civil Engineering, Jiangxi Institute of Construction, Nanchang, China

effect of damage threshold on rock damage evolution and combined it with statistical theory to develop a rock damage evolution equation. Jiang et al. [17] established a sandstone constitutive model under coupled water–rock action based on statistical strength theory and damage theory and carried out the applicability of the constitutive model through numerical tests and indoor tests. From the perspective of the energy released by rock damage, Zhou et al. [18] developed a damage constitutive model for rocks based on the image-only theory.

The above research results have analysed the deterioration of the mechanical properties of rocks under chemical corrosion, but relatively little research has been carried out on the functional relationship between mechanical parameters and damage parameters, and the study of the constitutive equations of rocks after prolonged corrosion still needs to be further explored. This paper takes red sandstone as the research object, sets up five corrosion stages, analyses the change law of mechanical parameters of red sandstone specimens after acid corrosion, combines the change of porosity, introduces chemical damage variables, establishes the functional relationship between mechanical parameters and chemical damage variables, and derives the change law of mechanical properties of red sandstone after acid corrosion. Based on the characteristics of the uniaxial compression stress–strain curve and the Lemaitre strain equivalence principle, combined with the Weibull distribution statistical damage model for micro-fractures and porosity change after acid corrosion, and considering the effect of the compression-dense section, the constitutive equations of the red sandstone were obtained by segmentation.

Due to the wide range of applications of red sandstone in real geotechnical engineering field, its mechanical properties have a direct impact on the design parameters of the engineering. However, the corrosion of red sandstone caused by acid rain and groundwater can lead to changes in its physical properties and mechanical parameters, which in turn affects the safety and stability of the engineering

projects. Therefore, studying the mechanical properties and constitutive model of red sandstone under acid corrosion are important for understanding and predicting its behaviour in corrosive environments, and for improving the accuracy and reliability of engineering design. Additionally, investigating the effect of acid corrosion on the mechanical properties of sandstone can help assess the durability and safety of red sandstone, ensuring the long-term stability and safe operation of engineering projects.

Test Material and Methods

The test rock samples were taken from a road tunnel project and to reduce the influence of variability in the test results, all red sandstone was taken from the same rock mass. The main minerals of the red sandstone were identified by X-ray diffraction (XRD) as quartz (SiO_2), calcite ($CaCO_3$), potassium feldspar ($KAlSi_3O_8$), calcium feldspar ($CaAl_2Si2O_8$) and sodium feldspar ($NaAlSi3O8$). Standard cylindrical specimens of 50mm diameter and 100mm height are produced in accordance with the International Society for Rock Mechanics (ISRM) test protocols. The density of the dried sample was determined to be 2.634 g/cm^3 with an initial porosity of 2.27%. Given the complexity of acidic conditions in nature, and taking into account weak, medium and strong acids, sulphuric acid was chosen to simulate an acidic environment. The pH values of the acidic solutions were set at 5, 3, and 1, respectively. Rock specimens and acid equipment are shown in Fig. 1.

To obtain satisfactory corrosion results, each stage was set for 30d, divided into 5 stages, and the solution was replaced after each stage of corrosion, with the pH of the replacement solution remaining the same as before. The test simulates the corrosion effect of red sandstone in an acidic environment, using different pH acid solutions and corrosion time as variables, in a group of three rock samples, for a total of 18 groups. In the natural state (0d),

Fig. 1 Rock specimens and acid equipment **a** Rock specimens; **b** acid equipment

(a)　　　　　　　　　　　　　　(b)
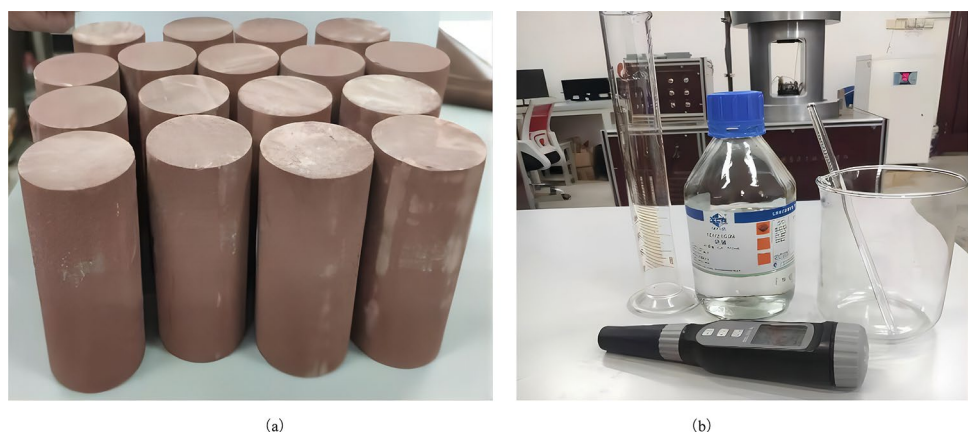
Fig. 2 ZTRE-210 microcomputer-controlled three-axis rock tester

stage 1 (30d), stage 2 (60d), stage 3 (90d), stage 4 (120d) and stage 5 (150d), three specimens from each group were removed and the mass of the specimens in the wet saturated state and after drying at 105 °C for 48 h was measured and the dried specimens were subjected to uniaxial compression tests. The uniaxial compression test uses the ZTRE-210 microcomputer-controlled triaxial rock tester with displacement control, as shown in Fig. 2.

Three rock samples were selected under different maintenance conditions and their mechanical parameters were determined by uniaxial compression test, and the rock samples with the compressive strength closest to the mean value were selected as the analysed samples in each group.

Results of the Tests and Analysis

Red Sandstone Porosity Changes during Acid Corrosion

As the red sandstone samples are corroded by the acid solution, the mineral composition is altered and partially dissolved in the acid solution, increasing the porosity of the samples. At the end of each stage of corrosion, the mass of the specimen in the wet saturated state and after drying at 105 °C for 48 h was determined. Since the difference between the weight of the sulphuric acid solution and the weight of water is not significant, the weight of the sulphuric acid solution at different pH values is taken as 1g/cm3 in the calculation. In order to study the variation pattern of porosity at different stages of corrosion, the expressions for the porosity and secondary porosity of the specimen are defined as follows:

$$n_t = \frac{M_t - m_t}{\rho V} \times 100\% \tag{1}$$

$$\Delta n = n_t - n_0 \tag{2}$$

In the formula, n_t is the porosity after stage t corrosion, M_t is the mass in the wet saturated state after stage t corrosion, m_t is the mass in the drying state after stage t corrosion, ρ is the solution density, V is the volume after stage t corrosion, Δn is the secondary porosity, and n_0 is the porosity in the initial state.

The porosity and secondary porosity of the specimens at the end of each corrosion stage are shown in Table 1.

As can be seen from Table 1, in the first stage of the test corrosion, solution pH = 1, the increase in secondary porosity accounted for 62.26% of the total corrosion stage secondary porosity; solution pH = 3, the increase in corrosion stage secondary porosity; solution pH = 5, the increase in secondary porosity accounted for 66.15% of the total corrosion stage secondary porosity. It shows that the acid solution has a significant effect on the corrosion of the red sandstone specimens; for the same pH value, the secondary porosity increases with increasing corrosion time, but the trend of increase becomes slower. At the same corrosion stage, the secondary porosity gradually decreases after corrosion by acid solutions of pH = 1,3,5. This indicates that the stronger the acidity, the greater the secondary porosity and the more obvious the corrosion of the red sandstone specimens at the same maintenance stage.

According to the change rule of secondary porosity of red sandstone samples at different stages under acid solution, the

Table 1 Porosity and secondary porosity after each stage of corrosion

Solution pH	Corrosion time t/d	Porosity after corrosion n_t /%	Secondary porosity Δn/%
pH = 1	30	4.53	2.26
	60	5.33	3.06
	90	5.55	3.28
	120	5.73	3.46
	150	5.90	3.63
pH = 3	30	4.45	2.18
	60	5.18	2.91
	90	5.35	3.08
	120	5.51	3.24
	150	5.62	3.35
pH = 5	30	4.40	2.13
	60	5.10	2.83
	90	5.26	2.99
	120	5.39	3.12
	150	5.49	3.22

change of secondary porosity of samples can be fitted by the following equation:

$$\Delta n = Ae^{-Bx} + C \tag{3}$$

where A, B and C are the fitted parameters of the secondary porosity. The fitted curve is shown in Fig. 3, and the parameters are given in Table 2.

As can be seen from Fig. 3, the secondary porosity gradually increased as the corrosion time increased, with the first two stages increasing most markedly, the last three stages increasing more slowly and finally stabilising.

Uniaxial Compression Test

The uniaxial compressive stress–strain curves of the specimens under different acid corrosion conditions are divided into the compression-tight stage, the elastic stage, the plastic stage, and the destruction stage, as shown in Fig. 4. The peak compressive strength is the ultimate load value of the specimen at the time of destruction, the corresponding strain is the peak strain, and the elastic modulus is the slope of the elastic stage.

The stress–strain curves of rock samples under different corrosion conditions are shown in Fig. 5. According to the stress–strain curve of the specimen, the relevant mechanical parameters were obtained and the mechanical parameters at each stage are shown in Fig. 6.

As can be seen from Figs. 5 and 6, the compressive strength and elastic modulus gradually decrease, and the peak strain gradually increases as the corrosion stage increases for the same pH acid solution corrosion. Analysis of the changes in the mechanical parameters of the red sandstone specimens after corrosion with acid solution at pH = 1 showed that the compressive strength after the first

Table 2 Values of the fitted parameters

| Solution pH	Fit parameter A	Fit parameter B	Fit parameter C
pH = 1	− 3.55	0.032584	3.56
pH = 3	− 3.29	0.035386	3.29
pH = 5	− 3.17	0.036603	3.17

stage of corrosion was 56.68 MPa, a decrease of 19.61% compared to the natural conditions; the compressive strength after the fifth stage of corrosion was 46.16 MPa; a decrease of 34.53% compared to the natural conditions. After the first stage of corrosion, the modulus of elasticity was 16.24 GPa, a decrease of 60.43% compared to natural conditions; after the fifth stage of corrosion, the modulus of elasticity was 11.28 GPa; a decrease of 75.20% compared to natural conditions. After the first stage of corrosion, the peak strain was 4.84; an increase of 46.22% compared to natural conditions; after the fifth stage of corrosion, the peak strain was 6.02, an increase of 81.87% compared to natural conditions. The mechanical parameters change in the same pattern after corrosion by acid solutions of pH = 3 and 5.

Analysis of changes in mechanical parameters of red sandstone specimens after corrosion by acid solutions of different pH at the same corrosion stage: the more acidic the solution, the lower the compressive strength and elastic modulus and the larger the peak strain.

To further explore the relationship between the mechanical parameters of the specimens, the pH of the acid solution and the corrosion stage, curves were fitted to the variation patterns of compressive strength, elastic modulus, and peak strain. The fitted curves are shown in Fig. 7:
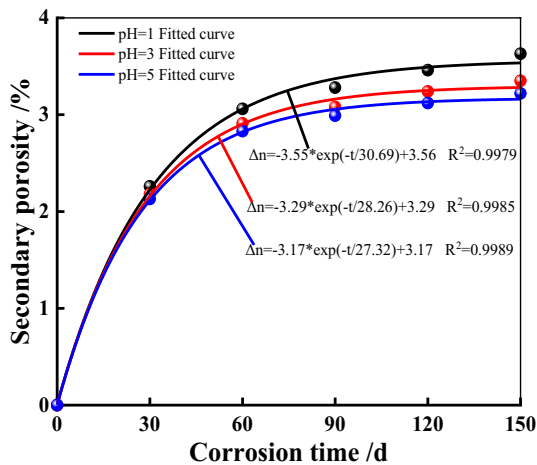
Fig. 3 Curves of secondary porosity with corrosion time
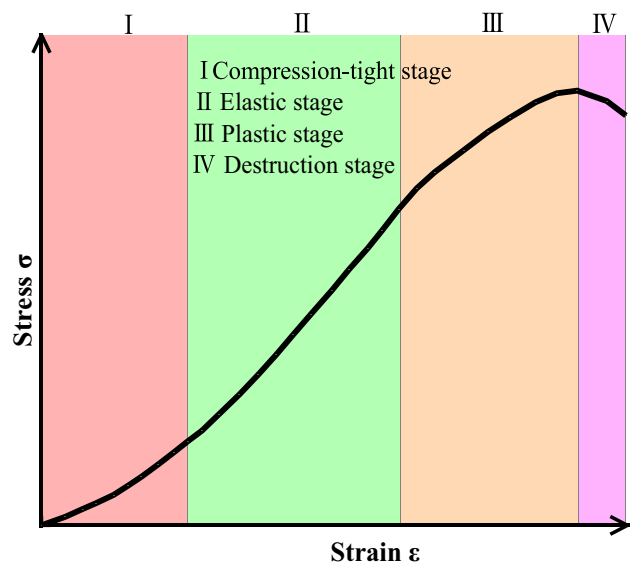
Fig. 4 Typical stress–strain curve under uniaxial compression
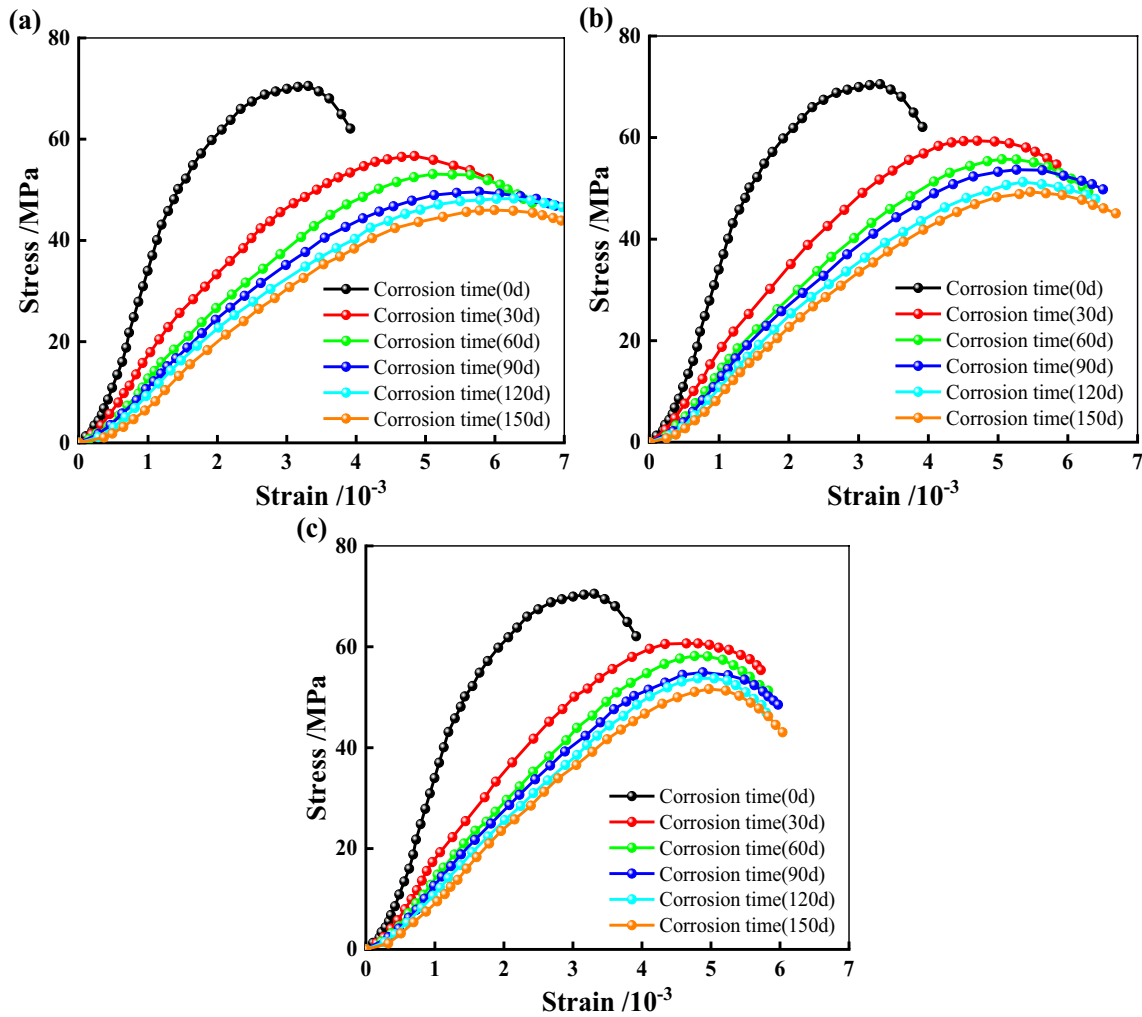
Fig. 5 Stress–strain curves of rock samples under different corrosion condition **a** pH = 1; **b** pH = 3; **c** pH = 5

As can be seen from Fig. 7, with the increase in corrosion stage, the mechanical parameters of the specimen are a regular change. Compressive strength and elastic modulus change in the same trend, the longer the corrosion time, the lower the pH of the solution, the greater the decrease in value, but the degree of decrease gradually decreases and finally, tends to a stable value. For the change in peak strain, the longer the corrosion time and the lower the pH of the solution, the greater the peak strain, but the rate of increase decreases, again tending towards a stable value at the end.

Effect of Chemical Damage on Mechanical Parameters

As the red sandstone specimen is corroded by the acid solution, the quality of the specimen will change due to the chemical reaction between the acid and the minerals, and the minerals will be continuously precipitated out, causing a change in the porosity of the specimen, and the change in

porosity will lead to a change in the mechanical parameters. In order to quantify the relationship between compressive strength and elastic modulus and porosity change, a chemical damage variable was introduced and, combined with the secondary porosity fitted in the previous part of the article, the damage variable was described by the expression:

$$D_c = \Delta n / (1 - n_0) = (Ae^{-Bx} + C)/(1 - n_0) \tag{4}$$

where A, B, C are secondary porosity fit parameters.

The fitted curves are shown in Fig. 8, and the chemical damage variables were fitted to compressive strength and elastic modulus, respectively.

As can be seen from Fig. 8, the compressive strength and elastic modulus of the red sandstone specimens vary regularly with chemical damage, and the mechanical properties of the specimens decrease significantly as the damage variables increase, with both compressive strength and elastic
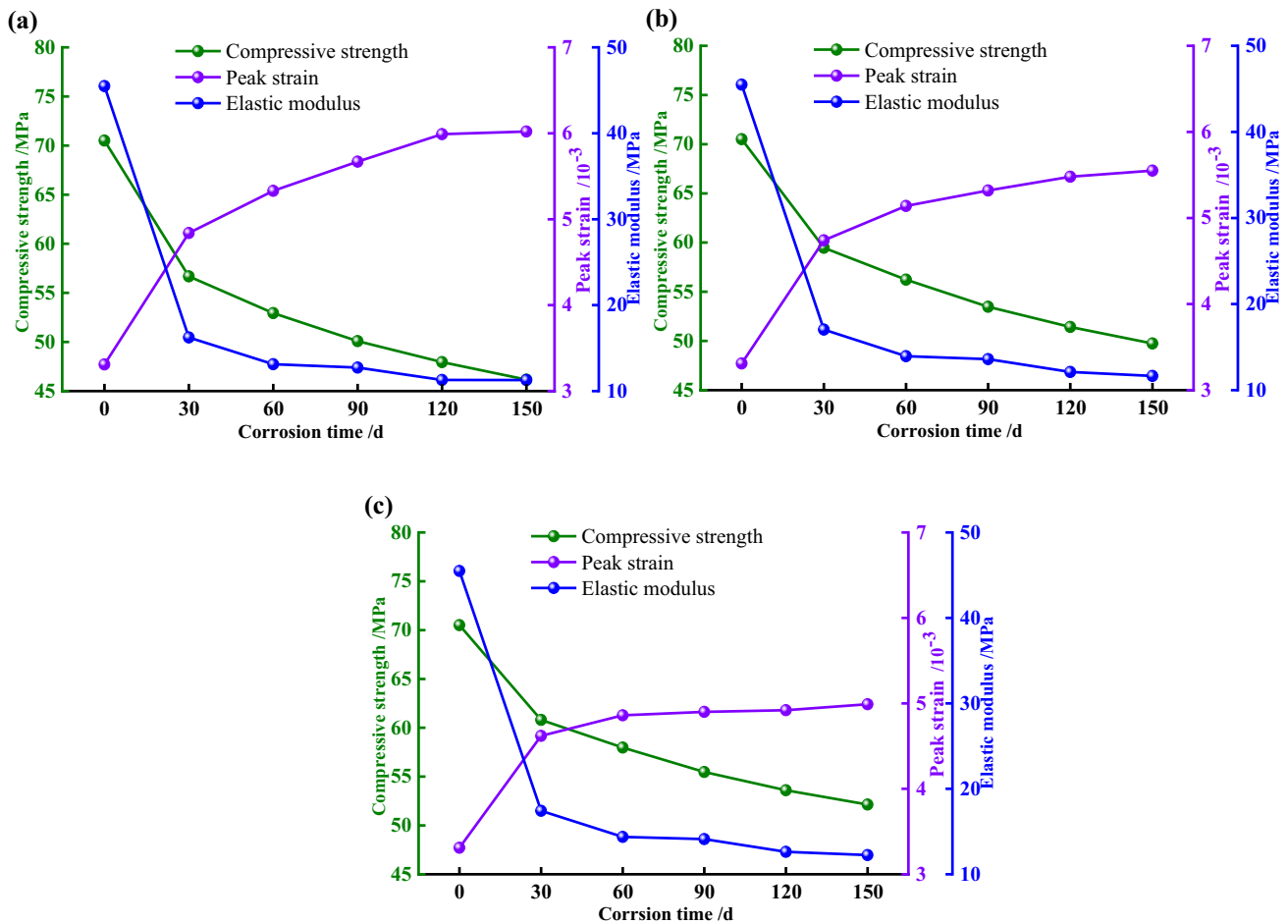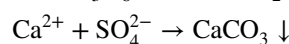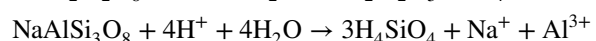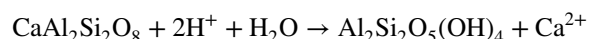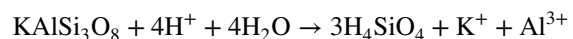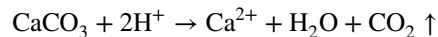
Fig. 6 Relationship curves of stress, strain, and elastic modulus of rock samples with corrosion condition **a** pH = 1; **b** pH = 3; **c** pH = 5

modulus decreasing. This indicates that the accumulation of chemical damage causes changes in the mechanical properties of the red sandstone. The proposed functional relationship between chemical damage variables and mechanical parameters based on secondary porosity can help to assess the mechanical properties of red sandstone from the perspective of void fraction change.

## Mechanism of Red Sandstone Degradation under Acid Solution Corrosion

The deterioration of the mechanical properties of red sandstone after corrosion by acid solutions is a complex process resulting from a combination of physico-chemical effects. The mechanical properties of the rock are influenced by a combination of its mineral composition and the nature of the cement. The natural rock has a certain amount of voids, and the acid solution enters the voids and forms a film of water on the mineral particles, the presence of which increases the water pressure in the voids and reduces friction and contact between the particles.

The main mineral compositions of the red sandstone specimens are quartz (SiO_2), calcite ($CaCO_3$), potassium feldspar ($KAlSi_3O_8$), calcium feldspar ($CaAl_2Si_2O_8$), and sodium feldspar ($NaAlSi_3O_8$). The sulphuric acid solution contains large amounts of H^+ and $SO4^{2-}$ and produces the following chemical reactions during the corrosion phase:

$$CaCO_3 + 2H^+ \rightarrow Ca^{2+} + H_2O + CO_2 \uparrow$$
$$KAlSi_3O_8 + 4H^+ + 4H_2O \rightarrow 3H_4SiO_4 + K^+ + Al^{3+}$$
$$CaAl_2Si_2O_8 + 2H^+ + H_2O \rightarrow Al_2Si_2O_5(OH)_4 + Ca^{2+}$$
$$NaAlSi_3O_8 + 4H^+ + 4H_2O \rightarrow 3H_4SiO_4 + Na^+ + Al^{3+}$$
$$Ca^{2+} + SO_4^{2-} \rightarrow CaCO_3 \downarrow$$

As the chemical reaction progresses, the minerals in the rock are continuously dissolved and precipitated, the voids in the sample increase, the bond between the particles weakens and the mechanical properties deteriorate. In conclusion, red sandstone corroded by acid solutions is a combined physico-chemical effect with manifestations of increased porosity and reduced compressive strength and elastic modulus.

Fig. 7 Relationship between mechanical parameters and time of red sandstone specimens: **a** curves of compressive strength with corrosion time; **b** curves of elastic modulus with corrosion time; **c** curves of peak strain with corrosion time
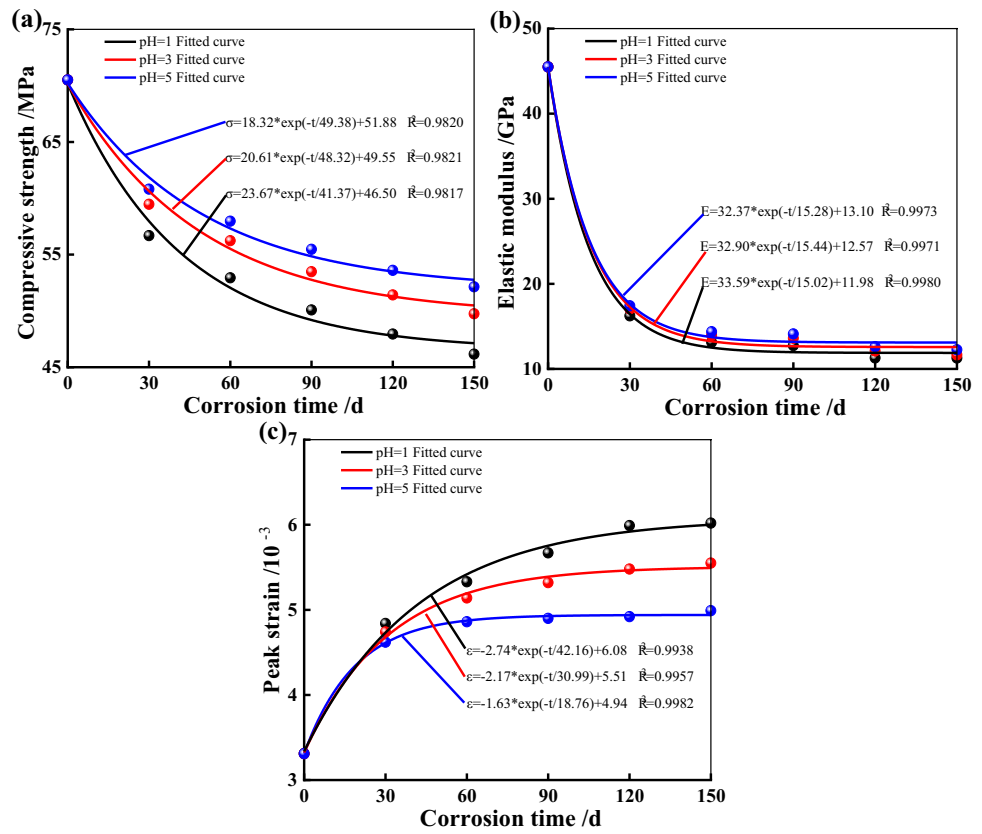
Fig. 8 Between mechanical parameters and damage variables of red sandstone specimens: **a** fitted curves of compressive strength of red sandstone versus chemical damage variable; **b** fitted curves of elastic modulus of red sandstone versus chemical damage variable
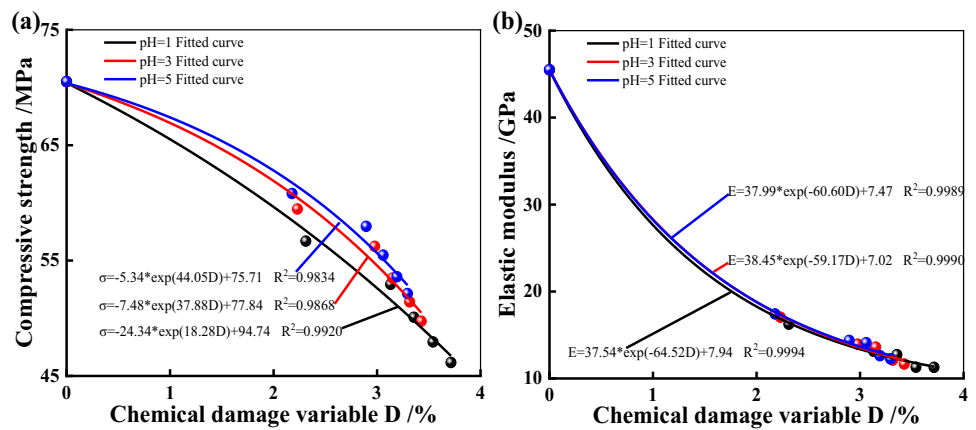
Red Sandstone Constitutive Model

Establishment of Constitutive Model

The red sandstone specimen is subjected to an axial load, from a microscopic point of view it can be divided into three parts: void, damaged, and undamaged, and the load is carried only by the undamaged part. The simplified mechanical model is shown in Fig. 9:

Assuming that the specimen is subjected to a nominal stress of σ_i and that the undamaged part is subjected to a

real stress of σ_i', it follows from the Lemaitre equivalence principle that:

$$\sigma_i A = \sigma_i' A_1 \tag{5}$$

$$\frac{\sigma_i}{\sigma_i'} = \frac{A_1}{A} = \frac{A - A_0}{A} \times \frac{A_1}{A_1 + A_2} = (1 - n) \times (1 - D) \tag{6}$$

A large number of microscopic defects are randomly distributed in the rock, and the defects can be considered as random damage. Based on a statistical damage mechanics
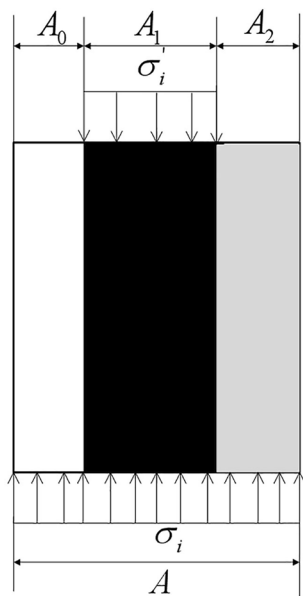
Fig. 9 Simplified microscopic stress model of acid corroded red sandstone element

approach to the study, it is assumed that the specimen micro-elements in uniaxial compression tests obey a Weibull distribution with a probability density function of:

$$P(\varepsilon) = \frac{m}{\varepsilon_0} \left(\frac{\varepsilon}{\varepsilon_0} \right)^{m-1} \exp \left[-\left(\frac{\varepsilon}{\varepsilon_0} \right)^m \right] \qquad (7)$$

where $P(\varepsilon)$ is the rock micro-element intensity distribution function; ε is the micro-element intensity random distribution variable; and m and ε_0 are the distribution parameters.

Assuming that the total number of micro-elements under load is N and the number of micro-elements with broken rings is n, the statistical damage variable D is given by:

$$D = \frac{n}{N} \qquad (8)$$

At a given strain ε, the number of ring-breaking micro-elements, n:

$$n = \int_0^\varepsilon NP(\varepsilon)d\varepsilon = N \left\{ 1 - \exp \left[-\left(\frac{\varepsilon}{\varepsilon_0} \right)^m \right] \right\} \qquad (9)$$

$$D = 1 - \exp \left[-\left(\frac{\varepsilon}{\varepsilon_0} \right)^m \right] \qquad (10)$$

By combining the above equations, the constitutive model of the damage under uniaxial compression is given by:

$$\sigma = E\varepsilon(1-n)(1-D) = E\varepsilon(1-n) \exp \left[-\left(\frac{\varepsilon}{\varepsilon_0} \right)^m \right] \qquad (11)$$

It has been shown that at low stresses, the fitted stress–strain curve is upwardly convex or approximately straight. After acid corrosion, due to the increased porosity of the specimen, when the stress level is low, there is an obvious pressure dense section with a downward concave curve, and the functional form of Eq. (10) cannot reflect the characteristics of the pressure dense section. According to the characteristics of the Weibull distribution function shape, the shape of the constitutive curve is mainly related to the $\exp[-(\varepsilon/\varepsilon_0)^m]$ in equation. According to the stress–strain depression characteristic of the compression-tight section, and changing this part of the constitutive equation to $\exp[-(\varepsilon/\varepsilon_0)^m]$, the constitutive equation of the compression-tight section is obtained, which can better reflect the characteristics of the compression-tight section. In this paper, using the above idea and considering the characteristics of the compacted section, the stress–strain curve at the end of the compacted section is assumed to be ε_{1c}, and the red sandstone segmental damage constitutive equation under acid corrosion is:

when $\varepsilon_1 \le \varepsilon_{1c}$:

$$\sigma = E\varepsilon(1-n)(1-D) = E\varepsilon(1-n) \left\{ 1 - \exp \left[-\left(\frac{\varepsilon}{\varepsilon_0} \right)^m \right] \right\} \qquad (12)$$

When $\varepsilon_1 > \varepsilon_{1c}$, the damage constitutive equation is in accordance with Eq. (11).

Determination of damage parameters

The key to establishing the above constitutive equations is the determination of the damage parameters m and ε_0. Usually, there are two methods for solving parameters in statistical models, one is the fitted parameter solving method, and the other is the peak point solving method. The physical meaning of the peak solving method is clear, but the solving process is complicated, the fitted method solves the process easily, and the fitting effect is better; this paper uses the fitted method to solve.

When $\varepsilon_1 \le \varepsilon_{1c}$, deforming the formula by moving the term given:

$$1 - \frac{\sigma_1}{E\varepsilon_1(1-n)} = \exp \left[-\left(\frac{\varepsilon_1}{\varepsilon_{01}} \right)^{m_1} \right] \qquad (13)$$

Taking the logarithm on both sides given:

$$\ln \left\{ 1 - \frac{\sigma_1}{E\varepsilon_1(1-n)} \right\} = -\left(\frac{\varepsilon_1}{\varepsilon_{01}} \right)^{m_1} \qquad (14)$$

A logarithmic transformation of the term results in the following equation:

$$\ln\left\{-\ln\left\{1-\frac{\sigma_1}{E\varepsilon_1(1-n)}\right\}\right\} = m_1\ln\varepsilon_1 - m_1\ln\varepsilon_{01} \quad (15)$$

Parametric equivalence substitution is performed for the equations, given:

$$Y = \ln\left\{-\ln\left\{1-\frac{\sigma_1}{E\varepsilon_1(1-n)}\right\}\right\}$$

$$X = \ln\varepsilon_1$$

$$b_1 = -m_1\ln\varepsilon_{01}$$

Thence:

$$Y = m_1 X + b_1 \quad (16)$$

A linear fit to the stress–strain curve data in the compression-tight region allows the constitutive equations in the compression-tight region to be solved to obtain the parameters m_1 and b_1, which given:

$$\varepsilon_{01} = \exp\left(-\frac{b_1}{m_1}\right) \quad (17)$$

When $\varepsilon_1 > \varepsilon_{1c}$, m_2 and ε_{02} can also be obtained after obtaining the pressure tight section as above.

Verification of Constitutive Equations

To verify the applicability of the constitutive equation, the specimens with the compressive strength closest to the average value in each group after corrosion by acid solution were selected as representative and solved by segmental fitting according to the stress–strain curves and the values of the parameters m and ε0 under the corrosive conditions of different acid solutions, as shown in Table 3.

The theoretical curve of this constitutive equation is obtained by substituting the solution parameters m and ε_0. The uniaxial compression test curve is analysed by comparison with the theoretical curve, as shown in Fig. 10.

As can be seen from Fig. 10, the theoretical curve of the constitutive equation established by segmentation has a high degree of agreement with the experimental curve, which confirms the adequacy of the constitutive equation and can better reflect the damage law of the red sandstone after corrosion by acid solution. As shown in Table 3, before the compaction-tight stage, the value of m_1 increases and the value of ε_{01} decreases with the increase in acidity of the corrosive solution and the increase in corrosive time. After the compaction-tight stage, the values of m_2 and ε_{02} are smaller with the increase in acidity of the conditioning solution and the increase in conditioning time. The trend of the fitted parameter m_2 in the second stage is consistent with the brittleness of the rock samples, and its physical meaning can be interpreted as an indicator of the brittleness of the rock, and

Table 3 Fitting results of test curves under different corrosion conditions

Solution pH		Fit parameters			
		$\varepsilon_1 \le \varepsilon_{1c}$		$\varepsilon_1 > \varepsilon_1$	
		m_1	ε_{01}	m_2	ε_{02}
pH = 1	30	0.5546	3.2356	4.5636	6.9029
	60	0.9646	3.0564	4.4579	6.7246
	90	1.2784	2.7764	3.2361	6.6030
	120	1.7445	2.5472	3.1107	6.3616
	150	2.2445	2.4672	3.0751	6.1937
pH = 3	30	0.5476	3.3466	5.8372	7.6770
	60	0.9524	3.1613	5.2861	7.5537
	90	1.2623	2.8716	4.0445	7.5155
	120	1.7225	2.6346	3.9395	7.0431
	150	2.2162	2.5518	3.8959	6.4137
pH = 5	30	0.5384	3.5484	8.2506	8.6745
	60	0.9364	3.3519	7.4678	8.566
	90	1.2411	3.0448	6.0153	8.1506
	120	1.6935	2.7934	5.9128	7.4532
	150	2.1789	2.7057	4.7499	6.7294

the larger the value of m_2, the greater the corresponding brittleness. The trend of the parameter ε_{02} is consistent with the compressive strength of the rock samples, and its physical meaning can be interpreted as an indicator of the degree of rock brittleness, and the larger the value of ε_{02}, the higher the corresponding compressive strength.

Conclusions

Compared with natural conditions, after corrosion by acid solution, the porosity of red sandstone specimens increased, the compressive strength and elastic modulus decreased, the peak strain increased, and the specimens gradually became less brittle. And the more acidic the solution, the longer the corrosion time, the more significant the above changes, indicating that the acid solution on the red sandstone corrosion effect is obvious.

The chemical damage variables determined from the porosity changes are closely related to the compressive strength and elastic modulus of the red sandstone specimens. The mathematical functional relationship established by fitting the chemical damage variables to the mechanical parameters of the specimens illustrates that the accumulation of damage will cause changes in the mechanical properties of the specimens. It helps to determine the mechanical properties of the specimens from the change in secondary porosity.

Analysis of the corrosion mechanism of red sandstone under acid solution shows that the deterioration of

Fig. 10 Uniaxial compressive stress–strain curves for red sandstone under acid corrosion: **a** pH = 1 conditions; **b** pH = 3 conditions; **c** pH = 5 conditions
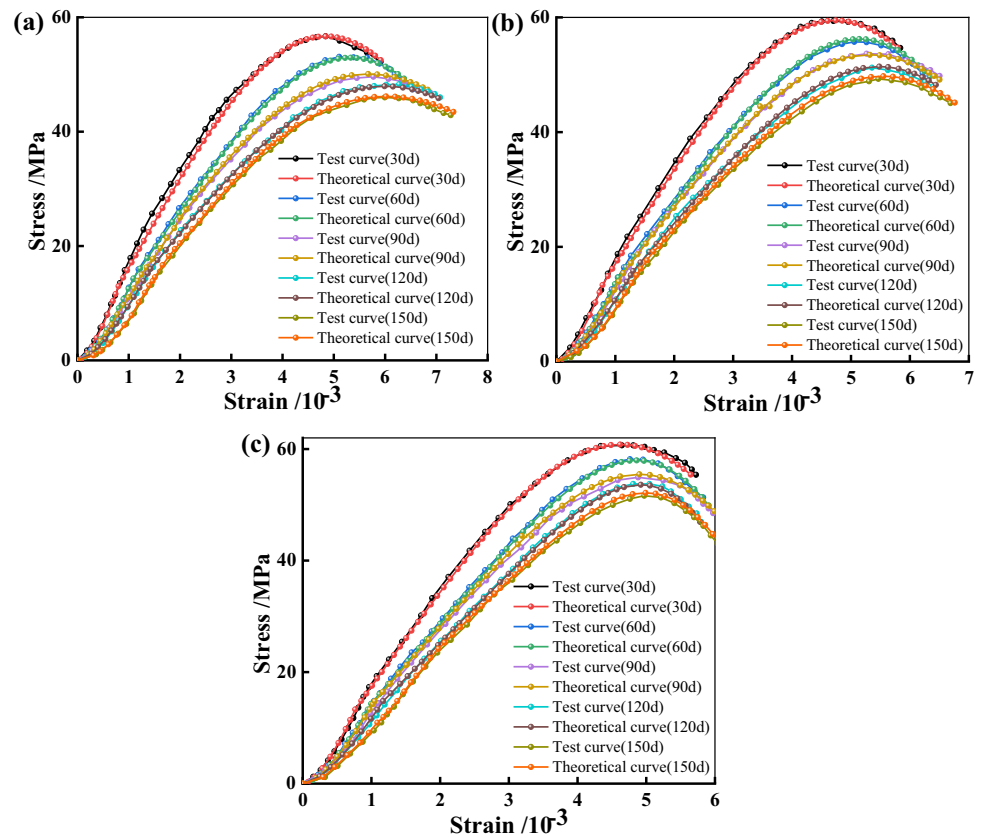
red sandstone specimens by acid solution is the result of both physical and chemical action. The physical effect is manifested by the formation of a water film in the mineral particles after the acid solution is immersed in the void of the specimen, resulting in a water pressure in the void and weakening the internal bond of the rock, whilst the chemical effect is specifically a chemical reaction between the mineral and the acid solution which dissolves and precipitates the mineral components of the rock, changing the composition of the solution and the specimen, increasing the porosity of the specimen and leading to the deterioration of the mechanical properties.

Based on the characteristics of stress–strain curves of red sandstone specimens under uniaxial compression after acid corrosion, the damage constitutive equation after acid corrosion was derived by considering the change of void ratio after acid corrosion, combining the Lemaitre strain equivalence principle with the Weibull distribution statistical damage model for micro-fractures. The influence of the compression-dense section was analysed, and the damage constitutive equation was segmented to derive the constitutive equation for red sandstone. The constitutive theoretical curve was compared with the experimental curve to verify the reasonableness of the constitutive equation.

Data availability The datasets generated during and/or analysed during the current study are available from the corresponding author on reasonable request.

Declarations

Conflict of interest On behalf of all authors, the corresponding author states that there is no conflict of interest.

References

1. Li L, Liu J, Xu X (2021) Study on the mechanical effect and constitutive model of montmorillonite under the action of acid rain: a case study on montmorillonite-quartz remolded soil. Adv Civ Eng 2021:6644411. https://doi.org/10.1155/2021/6644411
2. Mo Y, Zuo S, Wang L (2022) Mechanical characteristics of thick-bedded limestone with different bedding angles subjected to acid corrosion. Bull Eng Geol Environ 81:166. https://doi.org/10.1007/s10064-022-02667-2
3. Guo J, Mi X, Feng G, Qi T, Bai J, Wen X, Qian R, Zhu L, Guo X, Yu L (2022) Study on mechanical properties and weakening

mechanism of acid corrosion lamprophyre. Mater 15:6634. https://doi.org/10.3390/ma15196634

4. Han TL, Shi JP, Chen YS, Cao XS (2020) Salt solution attack-induced freeze-thaw mechanical degradation and its correlation with strength characteristic of mode-i fracture sandstone. Int J Geomech 20:04020039. https://doi.org/10.1061/(ASCE)GM.1943-5622.0001642

5. Han T, Shi J, Chen Y, Li Z (2016) Effect of chemical corrosion on the mechanical characteristics of parent rocks for nuclear waste storage. Sci Technol Nucl Install 2016:7853787. https://doi.org/10.1155/2016/7853787

6. Han T, Shi J, Chen Y, Cao X (2017) Physical and mechanical properties of marble under the combined effects of chemical solutions and freeze-thaw cycles. Geotech Tes J 40:1057–1070. https://doi.org/10.1520/GTJ20160225

7. Mei C, Fang Z, Wu W (2022) Slip transition of rock fractures due to chemical corrosion. Eng Geol 2022:106801. https://doi.org/10.1016/j.enggeo.2022.106801

8. Huang Z, Zeng W, Gu Q, Wu Y, Zhong W, Zhao K (2021) Investigations of variations in physical and mechanical properties of granite, sandstone, and marble after temperature and acid solution treatments. Constr Build Mater 307:124943. https://doi.org/10.1016/j.conbuildmat.2021.124943

9. Li S, Wu Y, Huo R, Song Z, Fujii Y, Shen Y (2021) Mechanical properties of acid-corroded sandstone under uniaxial compression. Rock Mech 54:289–302. https://doi.org/10.1007/s00603-020-02262-5

10. Chen F (2019) Three dimensional image of stress space geotechnical constitutive model. J Vis Commun Image Represent 60:398–406. https://doi.org/10.1016/j.jvcir.2019.03.012

11. Deng J, Cu D (2021) On a statistical damage constitutive model for rock materials. Comput Geosci 37:122–128. https://doi.org/10.1016/j.cageo.2010.05.018

12. Chen S, Qiao C, Ye Q, Khan MU (2018) Comparative study on three-dimensional statistical damage constitutive modified model of rock based on power function and Weibull distribution. Environ Earth Sci 77:108. https://doi.org/10.1007/s12665-018-7297-6

13. Li H, Xiong G, Zhao G (2016) An elasto-plastic constitutive model for soft rock considering mobilization of strength. Trans Nonferrous Met Soc China 26:822–834. https://doi.org/10.1016/S1003-6326(16)64173-0

14. Pan Y, Zhao Z, He L, Wu G (2020) A nonlinear statistical damage constitutive model for porous rocks. Adv Civ Eng 2020:8851914. https://doi.org/10.1155/2020/8851914

15. Ji M, Chen K, Guo H (2018) Constitutive model of rock uniaxial damage based on rock strength statistics. Adv Civ Eng 2018:5047834. https://doi.org/10.1155/2018/5047834

16. Li X, Cao W, Su Y (2012) A statistical damage constitutive model for softening behavior of rocks. Eng Geol 143:1–17. https://doi.org/10.1016/j.enggeo.2012.05.005

17. Jiang J, Hou Z, Hou K, Lu Y, Sun H, Niu X (2022) The damage constitutive model of sandstone under water-rock coupling. Geofluids 2022:1731254. https://doi.org/10.1155/2022/1731254

18. Zhou T, Qin Y, Ma Q (2020) Exploration of continuous rheological model for rock under uniaxial compression based on phenomenological damage theory. AIP Adv 10:105218. https://doi.org/10.1063/5.0026650